SIMULTANEOUS REFINEMENT OF TWO COMPONENTS
OF AN EXSOLUTION INTERGROWTH: CRYSTAL STRUCTURES
OF THE LINDSTRÖMITE – KRUPKAITE PAIR

Dan TOPA

Department of Materials Research, Division of Mineralogy, University of Salzburg, Hellbrunnerstr. 34, A–5020 Salzburg, Austria

Václav PETŘÍČEK and Michal DUŠEK

Institute of Physics, Acad. Sci.CR, Cukrovarnicka 10, CZ–162 53 Praha, Czech Republic

Emil MAKOVICKY[§]

Department of Geography and Geology, University of Copenhagen, Østervoldgade 10, DK–1350 Copenhagen K, Denmark

Tonči BALIĆ-ŽUNIĆ

Department of Geography and Geology, University of Copenhagen, Østervoldgade 10, DK–1350 Copenhagen K, Denmark

ABSTRACT

Crystal structures of intergrown lindströmite and krupkaite were determined in two distinct samples by a simultaneous crystal-structure refinement using a modified JANA program package. The exsolution intergrowths have a bulk composition, determined by means of electron microprobe, equal to $bd_{60.1}$ and $bd_{64.1}$, respectively. The subscript indicates a percentage of the aikinite component in this *bismuthinite derivative*. The crystal structure of lindströmite contains two aikinite-like ribbons $Cu_2Pb_2Bi_2S_6$ and eight krupkaite-like ribbons (ideally $CuPbBi_3S_6$) in a unit cell. The latter are oversubstituted; the ideally empty tetrahedral sites associated with them refined to the occupancy values of 0.04–0.09 Cu and 0.14–0.18 Cu, respectively, for the two above bulk compositions. The refined phase-compositions are $Cu_{6.26}Pb_{6.26}Bi_{13.74}S_{30}$ ($bd_{62.6}$) associated with $CuPbBi_3S_6$ (bd_{50}) for the sample 'bd$_{60}$' and $Cu_{6.64}Pb_{6.64}Bi_{13.36}S_{30}$ ($bd_{66.4}$) associated with oversubstituted krupkaite, the composition of which could not been refined, for the sample 'bd$_{64}$'. From stoichiometry calculations, the latter is ~bd_{60}. Both latter values may be somewhat overestimated as a result of cross-correlations between the two closely related structures during the refinement.

Keywords: lindströmite, krupkaite, crystal structure, simultaneous structure refinement, oversubstitution, bismuthinite–aikinite series.

SOMMAIRE

Nous avons déterminé de façon simultanée la structure cristalline de la lindströmite et de la krupkaïte en intercroissance dans deux échantillons distincts au moyen de l'ensemble de logiciels JANA. La composition globale de ces intercroissances, dues à l'exsolution, a été établie avec une microsonde électronique: $bd_{60.1}$ et $bd_{64.1}$, respectivement. Le chiffre en indice inférieur indique le pourcentage de la composante aikinite de ces dérivés de la bismuthinite. La structure de la lindströmite contient deux rubans semblables à l'aikinite, $Cu_2Pb_2Bi_2S_6$, et huit rubans semblables à la krupkaïte (de formule idéale $CuPbBi_3S_6$) par maille élémentaire. Ces derniers sont considérés sursubstitués, parce que leurs sites tétraédriques, normalement vides, montrent des taux d'occupation de 0.04–0.09 Cu et de 0.14–0.18 Cu *apfu*, respectivement, dans ces deux échantillons. Les compositions affinées sont $Cu_{6.26}Pb_{6.26}Bi_{13.74}S_{30}$ ($bd_{62.6}$) associé à $CuPbBi_3S_6$ (bd_{50}) pour l'échantillon 'bd$_{60}$', et $Cu_{6.64}Pb_{6.64}Bi_{13.36}S_{30}$ ($bd_{66.4}$) associé à la krupkaïte sursubstituée, dont la composition n'a pu être affinée, pour l'échantillon 'bd$_{64}$'. Selon la stoechiométrie, la composition de la krupkaïte sursubstituée serait ~bd_{60}. Dans les deux derniers cas de sursubstitution, les valeurs seraient légèrement surestimées à cause des intercorrélations dans l'affinement simultané de deux structures si étroitement semblables.

(Traduit par la Rédaction)

Mots-clés: lindströmite, krupkaïte, structure cristalline, affinement simultané de deux structures, sursubstitution, série bismuthinite–aikinite.

[§] *E-mail address*: emilm@geol.ku.dk

INTRODUCTION

The problem of simultaneous refinement of two or more crystal structures from overlapping diffraction patterns was solved and perfected for powder-diffraction data and is currently a part of all Rietveld refinement programs (Post & Bish 1989). In the realm of single crystals, the problem of oriented intergrowths with partially or fully overlapping reciprocal lattices has been successfully solved for twinned crystals, *i.e.* for one and the same crystal structure in two or more orientations. However, simultaneous refinement of two or more distinct structures in a single-crystal grain, in parallel or otherwise epitactically or topotactically determined orientations, and with heavily overlapping reciprocal lattices, poses additional problems in approach. It becomes necessary for the analysis and description of exsolution aggregates produced by the decomposition of the original (high-temperature) phase as well as for the analysis of intimate parallel intergrowths due to epitactic growth or replacement processes. Although separate treatments of the exsolved phases have been attempted in the past (*e.g.*, Makovicky & Skinner 1979, Horiuchi & Wuensch 1977), simultaneous refinement of such phases is a new procedure in single-crystal structure analysis.

The current problem involves a series of copper–lead–bismuth sulfides in which the exsolution phenomena are widespread, because the original continuous solid-solution (above ~300°C, Springer 1971) yields a large number of structurally ordered intermediate phases with restricted ranges of composition at ambient temperatures. As there is no general rule on how to make a complete separation of contributions from the two studied components, except for non-overlapping spots, a procedure similar to that used for a multiphase powder sample, *i.e.*, combining reflections from different domains, has been applied to this case. The JANA package of programs (Petříček *et al.* 2000), adapted to this kind of problem, was used in the present refinements.

LINDSTRÖMITE, KRUPKAITE AND THE BISMUTHINITE–AIKINITE SERIES

Lindströmite, ideally $Cu_3Pb_3Bi_7S_{15}$, and krupkaite, $CuPbBi_3S_6$, are two ordered structures of the bismuthinite–aikinite series (Bi_2S_3 – $CuPbBiS_3$). Structures of this series consist of M_4S_6 ribbons in a herringbone arrangement. The ribbons contain two distinct cation sites with a square-pyramidal 3 + 2 coordination, which becomes completed to monocapped trigonal coordination prisms where two additional atoms of sulfur from adjacent ribbons are involved. Such prisms include also pairs of lone electrons of the cations involved. The apical $M1$ positions invariably accommodate Bi; the central pair of $M2$ pyramids is a locus of incremental Pb-for-Bi substitution along the series. The latter is

connected with the incorporation of copper into adjacent tetrahedral voids.

At ambient temperature, the Bi_2S_3 – $CuPbBiS_3$ join consists of a series of ordered structures with the degree of (Cu + Pb)-for-(vacancy + Bi) substitution increasing by discrete increments [nine intermediate compositions have been recognized in the series (Topa *et al.* 2002a)]. These increments are materialized as distinct, ordered mixtures of three types of ribbons. Ribbon compositions Bi_4S_6 and $CuPbBi_3S_6$ mix in different proportions in the first half of the series, *i.e.*, the half that is poorer in copper, and $CuPbBi_3S_6$ ribbons mix with $Cu_2Pb_2Bi_2S_6$ ribbons in the second, Cu-enriched part. Ordered combinations of these ribbons result in 1-, 3-, 4-, and 5-fold superstructures of the fundamental, Bi_2S_3-like structure, which defines a subcell common to all of them. The exact composition of minerals belonging to the bismuthinite (Bi_2S_3) – aikinite ($CuPbBiS_3$) series is customarily expressed as the percentage of the aikinite component, *e.g,*. bd53 or 'krupkaite (53)', the remainder being the bismuthinite component. The symbol *bd* stands for *bismuthinite derivative*.

The definition of krupkaite (ideally), $CuPbBi_3S_6$ (*i.e.*, bd50), as a phase with a one-fold unit cell, space group $Pmc2_1$, comes from Žák *et al.* (1974), who also determined its structure. Another structure refinement was done by Mumme (1975). Lindströmite, ideally $Cu_3Pb_3Bi_7S_{15}$ (*i.e.*, bd60), is a five-fold superstructure, the first intermediate composition to follow after krupkaite on the Cu-rich side. Its history is somewhat complicated, reflecting the common occurrence of several macroscopically and microscopically indistinguishable members of the series and the difficulties in their recognition and separation for electron-microprobe and X-ray-diffraction studies. These problems were described in detail by Horiuchi & Wuensch (1977); the present-day crystallographic and compositional definition of lindströmite was introduced by Mumme *et al.* (1976).

Examination of the type material from Gladhammar, Sweden by HRTEM (Pring & Hyde 1987) revealed inhomogeneity in the type material, which consists of domains of krupkaite, lindströmite and hammarite, together with disordered regions. Similar investigations, however, proved the homogeneity of lindströmite from the Silver Miller mine, Ontario (Pring *et al.* 1998).

The crystal structure of lindströmite (in fact, "an ordering scheme for metal atoms") was determined in the space group $Pbnm$ from $hk0$ reflections as a projection on (001) (Horiuchi & Wuensch 1977). It was refined to $R_1 = 0.163$. Contributions from the estimated 6.3 vol.% krupkaite, present as a parallel exsolution-induced intergrowth, were subtracted using the data calculated from the structure of krupkaite refined by Mumme (1975). The structure of lindströmite was found to consist of $CuPbBi_3S_6$ and $Cu_2Pb_2Bi_2S_6$ ribbons combined in a ratio 4:1 but, at the above quoted R value, its details remained undetermined.

PROVENANCE AND CHEMICAL ANALYSES

The material studied comes from the metamorphosed scheelite (*i.e.*, tungsten) deposit of Felbertal, situated in the massif of the Hohe Tauern, Austria. Lindströmite occurs in the form of grains or as intergrowths with other sulfides in quartz veins parallel to the cleavage of the metamorphic rock. Detailed information on the mineralogy of the Felbertal deposit in relation to the bismuthinite–aikinite derivatives is given by Topa *et al.* (2002a).

The chemical composition of the crystals studied was obtained by electron-microprobe analysis before its extraction from a polished section. We used a JEOL–8600 electron microprobe equipped with Link EXL software with on-line ZAF correction. Analytical conditions employed were 25 kV and 30 nA; synthetic and natural sulfide standards were used. The averaged analytical results (wt.%) for 12 points on the crystal fragment $bd_{60.1}$ that was subsequently used for crystal-structure analysis, as well as for seven points on another structurally analyzed crystal of lindstömite from Felbertal ($bd_{64.1}$), which displays the maximal copper content measured, are presented in Table 1, together with the "ideal" simplified composition of lindströmite and krupkaite, and the composition derived from crystal-structure analysis.

CRYSTAL-STRUCTURE REFINEMENT

Theoretical part: multicomponent crystals

The diffraction pattern of crystals built from independently diffracting domains, having in general different structure and being differently oriented, is composed of diffraction spots of all contributing domains. Any diffraction spot belongs to at least one of the *n* reciprocal lattices in the diffraction pattern and can be indexed with three reciprocal vectors of the relevant domain. Thus the maximum number of reciprocal vectors to index all spots is *3n*. The relationship to the first arbitrarily chosen reference cell can be expressed by a reference matrix $\mathbf{T}_i$:

$$\begin{bmatrix} \mathbf{a}_{1i}^* \\ \mathbf{a}_{2i}^* \\ \mathbf{a}_{3i}^* \end{bmatrix} = \mathbf{T}_i \cdot \begin{bmatrix} \mathbf{a}_1^* \\ \mathbf{a}_2^* \\ \mathbf{a}_3^* \end{bmatrix} \qquad (1)$$

From the definition, it follows that the first matrix $\mathbf{T}_1$ is a unit one. As a recommendation, the reference reciprocal lattice should have the smallest possible reciprocal volume.

The current problem lies between the two theoretical limits of such a crystal, completely separated and completely overlapping lattices. Therefore, the set of $3n$ reciprocal vectors $\{\mathbf{a}_{1i}^*, \mathbf{a}_{2i}^*, \mathbf{a}_{3i}^*; i = 1, n\}$ can be reduced by the integer relationships that exist between some reciprocal vectors. The subset of non-overlapping reflections can help to find a partial solution, preceding a full refinement.

Principles of the calculation

The way how the crystal is composed from different domains, described by the equation (1) together with the assumption that diffraction in each domain takes

TABLE 1. CHEMICAL COMPOSITION AND FORMULA OF LINDSTRÖMITE AND RELATED PHASES

No.	mineral	N	Cu	Pb	Bi	Sb	S	Total	n_{aik}	Δn_{aik}	ev	Z
1	krupkaite	4	5.82(5)	19.3(1)	57.3(2)	0.10(1)	17.78(8)	100.3(3)	50.3	0.4	-0.25	1
2	oversubstituted krupkaite	6	6.65(9)	22.4(3)	53.2(5)	0.00	17.60(6)	99.9(3)	59.0	1.0	-1.19	1
3	lindströmite, crystal 1	12	6.85(4)	22.8(1)	52.8(1)	0.09(1)	17.5(1)	100.1(2)	60.1	0.7	-0.21	5
4	lindströmite, crystal 2	7	7.23(5)	24.2(1)	51.1(5)	0.00	17.53(7)	100.1(5)	64.1	0.9	-1.07	5
5	emilite	7	7.49(5)	24.9(1)	50.1(3)	0.00	17.48(9)	100.0(5)	66.4	0.7	-1.15	4
6	krupkaite bd_{50} (ideal)		5.83	19.01	57.51	-	17.65	100.00	50.0	0.0	0.0	1
7	"lindströmite" bd_{60} (ideal)		6.92	22.55	53.08	-	17.45	100.00	60.0	0.0	0.0	5
8	lindströmite $bd_{60.1}$ structure data		7.19	23.43	51.99	-	17.40	100.00	62.5	0.0	0.0	5
9	lindströmite $bd_{64.1}$ structure data		7.58	24.73	50.35	-	17.33	100.00	66.25	0.0	0.0	5

empirical formulae were calculated on the basis of Bi + (Pb+Cu)/2 = 8 atoms per formula unit (Me_6S_{12})

1) $Cu_{2.00} Pb_{2.03} Bi_{5.99} S_{12.04}$
2) $Cu_{2.32} Pb_{2.40} Bi_{5.64} S_{12.16}$
3) $Cu_{2.36} Pb_{2.43} Bi_{5.59} S_{12.04}$
4) $Cu_{2.53} Pb_{2.69} Bi_{5.44} S_{12.15}$
5) $Cu_{2.63} Pb_{2.68} Bi_{5.34} S_{12.15}$
6) $Cu_{2.96} Pb_{2.00} Bi_{6.00} S_{12.00}$
7) $Cu_{2.40} Pb_{2.46} Bi_{5.60} S_{12.00}$
8) $Cu_{2.59} Pb_{2.50} Bi_{5.50} S_{12.00}$
9) $Cu_{2.65} Pb_{2.65} Bi_{5.35} S_{12.00}$

The compositions are expressed in wt.%. N: number of analyses. Standard deviation for the last digit is shown in brackets. Calculation of the percentage of the aikinite component, n_{aik}, and the error of these calculations, Δn_{aik}, were performed according to Makovicky & Makovicky (1978). *ev* expresses the relative error in charge balance based on the sum of cation and anion charges. Z is *n*-fold superstructure of the fundamental subcell (Me_9S_{12}), common to all of them. Line 1 and 2 represent the compositions published in Topa *et al.* (2002). Line 5 is emilite, shown here for comparison with structure-refinement results on lindströmite '$bd_{64.1}$'. Lines 6 and 7 feature ideal compositions based on 12 sulfur atoms *p.f.u.* whereas lines 8 and 9 give results of structure refinement on the lindströmite component of the intergrowths studied.

place independently, lead to a general formula for the combined structure-factor $F(\mathbf{H})$, directly related to measured intensities:

$$F(\mathbf{H}) = \sqrt{[\nu_1 \, F_1^2 \, (\mathbf{H}{\bullet}\mathbf{T}_1) + ... + \nu_n \, F_n^2 \, (\mathbf{H}{\bullet}\mathbf{T}_n)]} \quad (2)$$

This relationship is based on the fact that the combined intensity is just a sum of individual contributions (squares of corresponding structure-factors). Individual volume-fractions ν_i related to the relative proportion of the ith domain are normalized to give a total equal to one. The individual structure-factors are calculated for each domain separately depending on the actual indices $\mathbf{H}{\bullet}\mathbf{T}_i$. As the relation matrices can generally be composed of real numbers or fractions, the scalar product $\mathbf{H}{\bullet}\mathbf{T}_i$ need not be an integer. Then the relevant contribution is equal to zero. Note also that each term in equation (2) can generally be calculated from the different structural model, which means that for a complete description, we need to know the set of relation matrices and also the structural correspondence. The approach to a multiphase crystal is just a natural generalization of the description used for twins. The main difference is that relation matrices need not be orthogonal to save the original metric properties, as all domains can have generally different lattices.

With the equation (2), one makes an additional assumption that the individual domains in the crystal have the same chance to diffract even for the cases when the crystal has appreciable absorption. This means that the method works properly for the cases where different domains (crystallites) are randomly distributed in the volume of the original crystal, a situation assumed to be valid in the intergrowths examined because of the homogeneity of microprobe-derived data on composition (Table 1) throughout the crystals.

Experimental and refinement data

The pre-analyzed crystals (Table 1) were extracted from a polished section as irregularly shaped fragments. A BRUKER AXS four-circle diffractometer equipped with CCD 1000K area detector was used (Table 2). The sample–detector distance was fixed at 8 cm. For the bd_{60} sample, 2880 static exposures 0.25° apart were made (the same number of exposures was used for the bd_{64} sample; data for this sample are given in parentheses). Each measurement lasted 60 (90 for the second sample) s, with 92% (93%) coverage inside the limits of the angular span covered. The SMART system of programs was used for unit-cell determination and data collection, SAINT+ for the calculation of integrated intensities, and SHELTX for the initial structure-solution and refinement (all Bruker AXS products). Empirical absorption-corrections (Table 2) were performed using program XPREP from the SHELXTL package. The merging factor R_{int} changed from 0.130 (resp. 0.108) to 0.097 (0.078) after this correction.

The current refinement was performed using the modified JANA2000 package. The starting structures were those calculated by Topa (2001) for krupkaite (bd_{50}) and the two samples of lindströmite, bd_{60} and bd_{64}, from Felbertal; the latter two samples are also the material and diffraction data used in the present investigations. The $\mathbf{T}_i$ matrices are [111] and [151] for lindströmite and krupkaite, respectively. Unlike the present refinements, the refinements of the lindströmite structures by Topa (2001) were undertaken with only the $hk0$ reflections, with $k = 5n$ and h,k odd (the non-overlapping reflections produced by krupkaite) eliminated and resulted in R equal to 0.11. The simultaneous refinement applied in the current study brought the R value down to 0.055 (0.086) and the relevant wR to 0.11 (0.17) for 2244 (2143) reflections having an intensity greater than $3\sigma(I)$. Refinement details are given in Table 2, atom parameters in Tables 3 through 6. Tables of observed and calculated structure-factors have been sent to the Depository of the Unpublished Data on the MAC web site [document Lindströmite CM46_525].

The degree of correlation between the two simultaneously refined structures and their reliability are reflected in the behavior of partially occupied copper sites. A refinement without constraints results in two different partly occupied Cu sites in lindströmite 'bd_{60}', which are supported by the indication of partial substitution of Bi by Pb in the relevant, adjacent Bi sites. It results in an empty tetrahedron plus a fully occupied Cu site in the admixed krupkaite; the latter is again supported by the absence of indications of Pb substitution in the adjacent Bi site. When, in an attempt to investigate this distribution more closely, fractional Cu occupancy was introduced into the empty tetrahedron of krupkaite, the agreement factor R became worse, and the fractional Cu4 site in lindströmite became unstable. The situation for 'bd_{64}' is more complicated; it is discussed below.

Another measure of the quality of the refinement is the comparison of selected global characteristics of the polyhedra (Balić-Žunić & Makovicky 1996, Makovicky & Balić-Žunić 1998) calculated for pure krupkaite (bd_{50}), which was refined by Topa et al. (2002b), and the present refinements of krupkaite, and for lindströmite without and with separation of the krupkaite contribution from the diffraction pattern. Tables 7 and 8 contain the principal interatomic distances, whereas Tables 9 and 10 contain characteristics of the polyhedra for the current refinements (for details, see the Discussion).

DESCRIPTION OF THE STRUCTURES

Lindströmite in bd_{60} and bd_{64}: the major component

The lattice parameters refined differ from the values a 4.010 Å, b 55.99 Å, and c 11.549 Å (our orientation) obtained by means of X-ray powder diffraction by Pring et al. (1998) and are closer to those given by Horiuchi & Wuensch (1977), a 4.001 Å, b 56.115 Å,

TABLE 2. LINDSTRÖMITE–KRUPKAITE INTERGROWTHS:
EXPERIMENTAL AND REFINEMENT DATA

	$bd_{60.1}$		$bd_{64.1}$	
Crystal data				
Chemical formula	$Cu_{2.38}Pb_{2.43}Bi_{5.59}S_{12.04}$	$Cu_2Pb_2Bi_6S_{12}$	$Cu_{2.53}Pb_{2.60}Bi_{5.44}S_{12.15}$	$Cu_2Pb_2Bi_6S_{12}$
Cell setting	Orthorhombic	Orthorhombic	Orthorhombic	Orthorhombic
Space group	$Pmcn$	$Pmc2_1$	$Pmcn$	$Pmc2_1$
a (Å)	4.0179(3)	4.0179	4.0206(4)	4.0206
b (Å)	56.141(4)=5×11.228	11.228	56.147(5)=5×11.229	11.229
c (Å)	11.5777(8)	11.578	11.586(1)	11.586
V (Å)^3	2611.6(3)		2615.4(4)	
Z	5		5	
D_x (Mg m^{-3})	7.009		7.0588	
Crystal form	irregular		irregular	
Crystal size (mm)	0.11 × 0.09 × 0.08		0.09 × 0.07 × 0.03	
Crystal color	metallic gray		metallic gray	
Data collection				
Diffractometer	Bruker CCD		Bruker CCD	
Detector–sample distance (mm)	80		80	
Number of frames	2880		2880	
Width of frames (°)	0.25		0.25	
Measurement time (s)/frame	60		90	
R_{int} (before corr.)	0.1302		0.1078	
R_{int} (after corr.)	0.0971		0.0783	
T_{min}/T_{max}	0.00092/0.01257		0.00037/0.01338	
Measured reflections	14669		14815	
Unique reflections	4448		3859	
Observed reflections	2243		2143	
Criterion for obs. reflections	$I > 3\sigma(I)$		$I > 3\sigma(I)$	
R_{int} for observed reflections	0.0566		0.0863	
θ_{min} / θ_{max} (°)	1.45/29.34		1.45/29.28	
Range of h,k,l	-5 < h < 3		-4 < h < 2	
	-75 < k < 70		-77 < k < 77	
	15 < l < 13		15 < l < 13	
Coverage (to Θ_{max})	92%		93%	
Refinement				
Refinement on	F^2		F^2	
R, wR (observed reflections)	0.0545/0.1070		0.0856/0.1680	
S	2.29		3.77	
No. of parameter	131		131	
Weighting scheme	$w = [\sigma^2(F) + (0.02F)^2]^{-1}$		$w = [\sigma^2(F) + (0.02F)^2]^{-1}$	
$(\Delta/s.u.)_{max}$	0.402		0.0431	
$\Delta\rho_{max}$ (eÅ^{-3})	9.29		7.73	
$\Delta\rho_{min}$ (eÅ^{-3})	-11.35		-8.26	
Extintioncoefficient	none		none	
Volume fraction				
lindströmite/krupkaite	0.663(10)	0.337(10)	0.625(15)	0.375(15)
Source of scattering factors	International Tables for X-Ray Crystallography Vol. C (1992)			
Program solution	SHELXS-97 (Sheldrick 1990)			
Program refinement	JANA2000 (Petříček et al. 2000)			

and c 11.5695 Å. The orthorhombic space-group *Pmcn* has been confirmed.

The crystal structure of lindströmite (Figs. 1, 2) contains seven independent Bi positions, three Pb sites, three major and two minor Cu sites, Cu4 and Cu5, with an indication of corresponding amounts of Pb substitution in the Bi sites adjacent to the minor Cu sites. The fifteen independent sulfur sites present were refined with isotropic displacement parameters.

Using the classical description of the phases belonging to the bismuthinite–aikinite series (Ohmasa & Nowacki 1970), the crystal structure of stoichiometric lindströmite contains eight krupkaite-like ribbons $CuPbBi_3S_6$ and two aikinite-like ribbons $Cu_2Pb_2Bi_2S_6$ in a unit cell. When, as an alternative, we use the modular description in which we delimit structural intervals between two adjacent (010) planes of tetrahedral voids

fully populated by copper, and name them according to the phases in which they occur in pure form, lindströmite contains paired krupkaite-like intervals (width

TABLE 3. POSITIONAL PARAMETERS AND B_{eq}/B_{iso} VALUES OF ATOMS IN THE LINDSTRÖMITE COMPONENT OF:

Atom	sof	x	y	z	B_{eq}/B_{iso}
			$bd_{60.1}$		
Bi1	1	0.25	0.03814(5)	0.0178(3)	0.0201(10)
Bi2	1	0.25	0.23742(5)	0.0226(3)	0.0173(9)
Bi3	1	0.25	0.43582(5)	0.0219(3)	0.0173(9)
Bi4	1	0.25	0.63477(5)	0.0178(3)	0.0173(9)
Bi5	1	0.25	0.83365(5)	0.0156(3)	0.0170(9)
Bi6	1	0.25	0.19232(4)	0.3477(2)	0.0186(7)
Bi7	1	0.25	0.39133(4)	0.3467(2)	0.0213(8)
Pb1	1	0.25	0.60068(4)	0.3253(3)	0.0213(9)
Pb2	1	0.25	0.80008(4)	0.3226(2)	0.0187(8)
Pb3	1	0.25	0.99821(4)	0.3316(3)	0.0242(9)
Cu1	1	0.25	0.54248(11)	0.2342(7)	0.019(2)
Cu2	1	0.25	0.74212(10)	0.2256(6)	0.018(2)
Cu3	1	0.25	0.94125(11)	0.2283(6)	0.019(2)
Cu4	0.044(14)	0.75	0.658(2)	0.759(15)	0.02
Cu5	0.087(14)	0.75	0.6394(12)	0.259(8)	0.02
S1	1	0.25	0.1281(2)	0.0514(14)	0.009(3)
S2	1	0.25	0.3280(2)	0.0504(15)	0.019(4)
S3	1	0.25	0.5278(2)	0.0460(13)	0.009(3)
S4	1	0.25	0.7245(2)	0.0447(14)	0.018(4)
S5	1	0.25	0.9245(2)	0.0444(15)	0.017(4)
S6	1	0.25	0.0615(3)	0.2136(16)	0.022(4)
S7	1	0.25	0.2601(2)	0.2175(13)	0.008(3)
S8	1	0.25	0.4602(3)	0.2189(17)	0.026(4)
S9	1	0.25	0.6604(2)	0.2122(15)	0.011(3)
S10	1	0.25	0.8590(3)	0.2125(15)	0.017(4)
S11	1	0.25	0.1110(3)	0.3767(16)	0.018(4)
S12	1	0.25	0.3104(3)	0.3826(16)	0.021(4)
S13	1	0.25	0.5122(2)	0.3821(14)	0.012(4)
S14	1	0.25	0.7122(3)	0.3732(15)	0.021(4)
S15	1	0.25	0.9113(3)	0.3740(15)	0.018(4)
			$bd_{64.1}$		
Bi1	1	0.25	0.03861(7)	0.0173(3)	0.0492(13)
Bi2	1	0.25	0.23771(6)	0.0226(3)	0.0489(13)
Bi3	1	0.25	0.43583(6)	0.0223(3)	0.0494(14)
Bi4	1	0.25	0.63488(6)	0.0179(3)	0.0491(14)
Bi5	1	0.25	0.83357(7)	0.0161(3)	0.0501(14)
Bi6	1	0.25	0.19224(6)	0.3470(3)	0.0460(11)
Bi7	1	0.25	0.39118(6)	0.3453(3)	0.0484(12)
Pb1	1	0.25	0.60070(6)	0.3271(3)	0.0505(13)
Pb2	1	0.25	0.80018(6)	0.3221(3)	0.0433(11)
Pb3	1	0.25	0.99830(5)	0.3326(3)	0.0497(13)
Cu1	1	0.25	0.54266(15)	0.2358(8)	0.037(3)
Cu2	1	0.25	0.74206(13)	0.2252(6)	0.029(3)
Cu3	1	0.25	0.94187(15)	0.2317(8)	0.040(3)
Cu4	0.138(18)	0.75	0.6566(9)	0.760(4)	0.02
Cu5	0.181(19)	0.75	0.6412(6)	0.276(4)	0.02
S1	1	0.25	0.1273(3)	0.0482(17)	0.040(5)
S2	1	0.25	0.3276(4)	0.044(2)	0.066(6)
S3	1	0.25	0.5281(3)	0.0419(16)	0.036(4)
S4	1	0.25	0.7237(4)	0.0416(18)	0.051(5)
S5	1	0.25	0.9241(4)	0.0383(19)	0.054(6)
S6	1	0.25	0.0632(4)	0.2118(18)	0.049(6)
S7	1	0.25	0.2590(3)	0.2184(15)	0.033(4)
S8	1	0.25	0.4627(5)	0.222(3)	0.080(9)
S9	1	0.25	0.6604(3)	0.2110(15)	0.029(4)
S10	1	0.25	0.8588(5)	0.213(2)	0.071(7)
S11	1	0.25	0.1102(3)	0.3789(16)	0.037(5)
S12	1	0.25	0.3095(4)	0.3835(17)	0.046(5)
S13	1	0.25	0.5124(3)	0.3802(15)	0.034(5)
S14	1	0.25	0.7110(4)	0.3753(17)	0.046(5)
S15	1	0.25	0.9116(3)	0.3727(16)	0.041(5)

sof: site-occupancy factor.

TABLE 4. ANISOTROPIC DISPLACEMENT PARAMETERS OF ATOMS IN THE LINDSTRÖMITE COMPONENT OF:

Atom	U_{11}	U_{22}	U_{33}	U_{12}	U_{13}	U_{23}
			$bd_{60.1}$			
Bi1	0.023(2)	0.0250(12)	0.0125(16)	0	0	0.0018(10)
Bi2	0.0156(18)	0.0223(11)	0.0140(15)	0	0	0.0018(10)
Bi3	0.016(2)	0.0207(11)	0.0152(16)	0	0	0.0021(10)
Bi4	0.019(2)	0.0155(10)	0.0174(17)	0	0	0.0061(9)
Bi5	0.0159(19)	0.0154(10)	0.0198(16)	0	0	0.0052(9)
Bi6	0.0184(15)	0.0171(10)	0.0204(13)	0	0	0.0043(9)
Bi7	0.0210(16)	0.0187(11)	0.0242(14)	0	0	0.0034(10)
Pb1	0.0256(18)	0.0173(11)	0.0211(15)	0	0	-0.0022(10)
Pb2	0.0203(16)	0.0201(11)	0.0157(13)	0	0	-0.0010(9)
Pb3	0.0238(18)	0.0164(10)	0.0323(17)	0	0	-0.0005(10)
Cu1	0.013(5)	0.031(3)	0.013(4)	0	0	-0.002(3)
Cu2	0.017(5)	0.025(3)	0.011(4)	0	0	0.002(3)
Cu3	0.020(5)	0.027(3)	0.011(4)	0	0	-0.002(3)
			$bd_{64.1}$			
Bi1	0.052(3)	0.0450(16)	0.051(2)	0	0	-0.0011(13)
Bi2	0.048(3)	0.0452(16)	0.054(2)	0	0	0.0055(13)
Bi3	0.049(3)	0.0459(17)	0.054(2)	0	0	-0.0073(14)
Bi4	0.049(3)	0.0420(16)	0.056(2)	0	0	0.0092(13)
Bi5	0.046(3)	0.0432(16)	0.061(2)	0	0	0.0023(13)
Bi6	0.047(3)	0.0381(14)	0.0529(16)	0	0	0.0059(13)
Bi7	0.049(3)	0.0398(15)	0.0567(17)	0	0	0.0013(13)
Pb1	0.052(3)	0.0374(15)	0.062(2)	0	0	-0.0013(14)
Pb2	0.051(3)	0.0411(14)	0.0373(14)	0	0	0.0021(11)
Pb3	0.048(3)	0.0320(13)	0.069(2)	0	0	0.0092(13)
Cu1	0.033(7)	0.031(4)	0.048(5)	0	0	-0.003(3)
Cu2	0.035(7)	0.033(4)	0.020(3)	0	0	0.000(3)
Cu3	0.044(8)	0.031(4)	0.046(5)	0	0	0.001(3)

TABLE 5. POSITIONAL PARAMETERS AND B_{eq}/B_{iso} VALUES OF ATOMS IN THE KRUPKAITE COMPONENT OF:

Atom	sof	x	y	z	B_{eq}/B_{iso}
			$bd_{60.1}$		
Bi1'	1	0	0.4245(4)	0.0844	0.0191(13)
Bi2'	1	0.5	0.0642(4)	0.1191(7)	0.0207(13)
Bi3'	1	0.5	-0.2855(4)	-0.0551(5)	0.0307(11)
Pb1'	1	0	0.2467(4)	0.221(2)	0.0302(12)
Cu1'	1	0	-0.0396(9)	-0.1252(12)	0.037(4)
Cu2'	0	0.5	0.5612	0.3662	0.02
S1'	1	0	0.1932(16)	0.011(5)	0.011(5)
S2'	1	0.5	0.3001(17)	-0.0178(19)	0.010(4)
S3'	1	0.5	-0.0576(17)	0.320(2)	0.012(4)
S4'	1	0	-0.1225(18)	0.058(2)	0.020(5)
S5'	1	0.5	0.6080(17)	0.145(2)	0.018(5)
S6'	1	0	0.5582(18)	-0.110(2)	0.015(5)
			$bd_{64.1}$		
Bi1'	1	0	0.4279(4)	0.0844	0.0273(15)
Bi2'	1	0.5	0.0688(4)	0.1208(4)	0.0271(15)
Bi3'	1	0.5	-0.2750(7)	-0.0593(7)	0.054(2)
Pb1'	1	0	0.2416(7)	-0.2278(7)	0.056(2)
Cu1'	1	0	-0.049(3)	-0.127(2)	0.080(10)
Cu2'	0	0.5	0.5612	0.3662	0.02
S1'	1	0	0.191(3)	0.222(3)	0.033(7)
S2'	1	0.5	0.309(3)	-0.017(3)	0.031(6)
S3'	1	0.5	-0.055(2)	0.320(2)	0.019(5)
S4'	1	0	-0.120(2)	0.050(2)	0.026(6)
S5'	1	0.5	0.6059(18)	0.1500(18)	0.017(4)
S6'	1	0	0.552(3)	-0.110(2)	0.027(6)

sof: site-occupancy factor.

TABLE 6. ANISOTROPIC DISPLACEMENT PARAMETERS OF ATOMS
IN THE KRUPKAITE COMPONENT OF:

Atom	U_{11}	U_{22}	U_{33}	U_{12}	U_{13}	U_{23}
			$bd_{60.1}$			
Bi1'	0.021(3)	0.0237(16)	0.013(2)	0	0	-0.0005(13)
Bi2'	0.026(3)	0.0222(16)	0.014(2)	0	0	0.0007(13)
Bi3'	0.037(2)	0.0335(17)	0.0211(17)	0	0	-0.0025(15)
Pb1'	0.036(3)	0.0324(16)	0.0218(18)	0	0	0.0096(14)
Cu1'	0.043(9)	0.045(5)	0.025(6)	0	0	0.003(5)
			$bd_{64.1}$			
Bi1'	0.022(4)	0.035(2)	0.0246(18)	0	0	-0.0039(17)
Bi2'	0.021(3)	0.039(2)	0.0214(17)	0	0	-0.0011(16)
Bi3'	0.029(4)	0.087(4)	0.045(3)	0	0	-0.020(3)
Pb1'	0.046(5)	0.068(4)	0.055(3)	0	0	0.032(3)
Cu1'	0.080(19)	0.115(19)	0.046(9)	0	0	0.002(10)

~11.2 Å each), which alternate with a single aikinite-like interval (width ~5.7 Å) (Fig. 2). In the present, slightly oversubstituted case of lindströmite with the total composition bd_{60}, the aikinite-like ribbon at y = 0 and ½ is intermeshed on both sides with slightly oversubstituted krupkaite-like ribbons which, in turn, are intermeshed with more intensely oversubstituted krupkaite-like ribbons centered at $y \approx 0.2$ and 0.3 (Fig. 2). The Cu4 and Cu5 positions belong respectively to these two types of oversubstitution. The same type of oversubstitution is found in lindströmite with the total composition bd_{64}, but both fractionally occupied Cu sites have higher, and about equal, occupancy in this lindströmite structure (Table 3).

The good quality of the joint refinement is revealed by a consistency of interatomic distances (Table 7) (values for 'bd_{60}' precede the bracketed values for 'bd_{64}'). Bismuth atoms in the marginal portions of the ribbons, Bi1–Bi5, have the shortest Bi–S distances, between 2.591 and 2.671 Å (2.556 – 2.750 Å for bd_{64}), accompanied by a pair of short Bi–S distances, 2.670 – 2.739 Å (2.681 – 2.764 Å for bd_{64}). The central Bi atoms Bi6 and Bi7 have a Bi–S distance to the vertex of the BiS_5 coordination pyramid equal to 2.609 Å (2.554 – 2.583 Å), and the opposing longer distances, to the adjacent ribbon, are equal to 3.438 Å (3.426 – 3.435 Å). The pairs of opposing Bi–S distances in the base of these pyramids range from 2.780 Å opposed by 2.975 to 2.793 Å opposed by 3.016 Å (2.776 Å opposed by 2.978 Å and 2.791 Å opposed by 3.037 Å in bd_{64}). Both central Bi atoms have coordinations slightly larger than the corresponding Bi3 site in krupkaite (bd_{50}), although smaller than the same site in krupkaite bd_{59}, which contains 0.09 Pb and exhibits M–S distances of 2.614 Å, 2 × 2.795 Å, 2 × 2.988 Å and 2 × 3.446 Å (Topa et al. 2002b).

The three Pb sites have typical Pb–S bond distances; averages of three shortest distances are 2.905, 2.934, and 2.938 Å (2.888, 2.979, and 2.919 Å) respectively, for Pb1, 2 and 3. Three fully occupied copper sites, Cu1, 2 and 3, have slightly asymmetric tetrahedral coordina-

tions, typical of bismuthinite–aikinite derivatives. The shortest Cu–S bonds lie in the interval 2.316 – 2.330 Å (2.321 – 2.377 Å), intermediate bonds between 2.343 and 2.354 Å (2.354 – 2.395 Å), and the longest bonds between 2.382 and 2.413 Å (2.395 – 2.460 Å). With the U_{iso} values fixed to 0.02, which is an average of U_{eq} values of Cu1–Cu3, the occupancy of Cu4 refined to 0.04 apfu and that of Cu5 refined to 0.09 apfu in bd_{60} and to 0.14 and 0.18 apfu, respectively, for the same sites in bd_{64}. For these sites, the lowest values from among the apparent Cu–S distances, which range from 2.238 to 2.416 Å (2.168 – 2.503 Å), reflect the fact that in over 80–95% of the cases, we deal with a tetrahedral void and not a CuS_4 tetrahedron.

Krupkaite: the minor component

For the minor phase of the intergrowth, krupkaite, the lattice parameters could not be refined independently, the bulk of its reflections being masked by those of lindströmite. Instead, those of stoichiometric krupkaite bd_{50}: a 4.015 Å, b 11.202 Å, c 11.560 Å, and those of oversubstituted krupkaite bd_{59}: a 4.021 Å, b 11.232 Å, c 11.581 Å were used, respectively. The crystal structure of krupkaite in 'bd_{60}' converged to a stoichiometric composition $CuPbBi_3S_6$ in a refinement without constraints, because the alternative copper site at x 0.5, y 0.5612, and z 0.3662, known from oversubstituted krupkaite (Topa et al. 2002b), refined to zero occupancy. Fractional atom-coordinates of the structures refined in the present procedure are very close to those of pure stoichiometric krupkaite. Differences in fractional coordinates (Table 5) with respect to the latest refinement of this phase by Topa et al. (2002b) are at or below 0.01 for all cations. These differences reach 0.05 Å when interatomic distances are considered (Table 8) (corresponding differences are 0.07 Å for the bd_{64} material). They represent five times the average value of the estimated standard error of bond lengths. With respect to pure krupkaite bd_{50} (Topa et al. 2002b), differences in bond lengths of krupkaite in 'bd_{60}' are mixed for all cation polyhedra (Table 8), which is also reflected in the similarity of their polyhedron characteristics.

DISCUSSION

Phase composition

The refined compositions of the phases are $Cu_{6.262}$ $Pb_{6.262}Bi_{13.738}S_{30}$ ($bd_{62.62}$) associated with $CuPbBi_3S_6$ (bd_{50}) for the sample 'bd_{60}' and $Cu_{6.638}Pb_{6.638}Bi_{13.362}S_{30}$ ($bd_{66.38}$) associated with oversubstituted krupkaite, the composition of which could not been refined. From stoichiometry calculations given below, its composition must be ~bd_{60}. Both latter values apparently are overestimated; the phase closest to lindströmite from the side of increasing substitution is a four-fold derivative, emilite, $bd_{66.4–67.5}$ (Topa et al. 2002a), with the lower
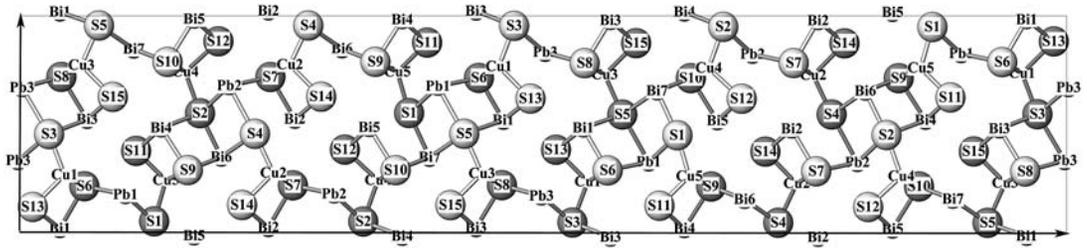
FIG. 1.   Atom labels for the crystal structure of lindströmite from the sample 'bd$_{60.1}$'. Projection on (100), *b* axis horizontal, *c* axis vertical. Shading indicates atoms at *x* = 0.25 and *x* = 0.75, respectively.
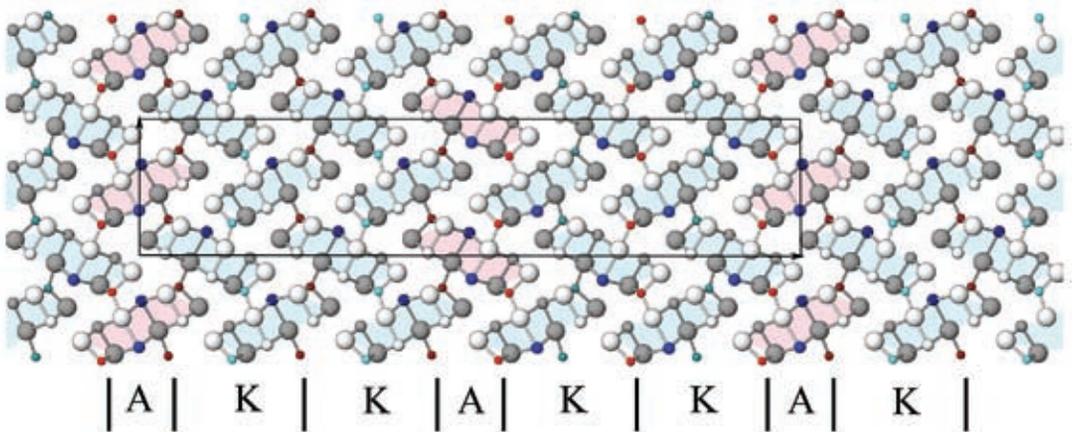

FIG. 2.   Crystal structure of lindströmite in projection on (100); *b* axis is horizontal. Atoms at two *x* levels, 2 Å apart are discerned by shading. Large white spheres: S, small white spheres: Bi and (Bi,Pb), black spheres: Pb, red spheres: fully occupied Cu sites, blue spheres: partly occupied Cu sites. Aikinite-like ribbons are indicated by a pink infill, (slightly oversubstituted) krupkaite-like ribbons by a light-blue infill. Boundary planes between aikinite (A) and krupkaite (K) modules indicated below the figure run through the slightly warped (010) planes of fully occupied coordination-tetrahedra of copper.

limit practically identical to the substitution percentage obtained for lindströmite in the present study.

Polyhedron characteristics

Plots of the volume of a sphere circumscribed to the coordination polyhedron of a large cation, or of the polyhedron volume itself, *versus* eccentricity of the position of this cation in its polyhedron, and plots of bond-valence values for these polyhedra, were found to offer the best means of evaluation of the refinement results. The circumscribed sphere is fitted to the polyhedron formed by ligands by a least-squares procedure, and the eccentricity value used is the distance of the cation from the center of the sphere, normalized to the radius of the sphere (Balić-Žunić & Makovicky 1996, Makovicky & Balić-Žunić 1998). Bond-valence values

were calculated using the constants derived by Brese & O'Keeffe (1991). The polyhedron characteristics are summarized in Tables 9 and 10.

Differences in oversubstitution notwithstanding, both lindströmite structures participate in the same clusters of characteristic polyhedron values in Figure 3. The Pb sites (Pb1 and 2) of krupkaite-like chains are separated in the plot from the largest Pb3 polyhedra of the aikinite-like chains. Among the coordination polyhedra of lead, the Pb1 polyhedron of lindströmite bd$_{64}$ exhibits the smallest volume and a large eccentricity, resulting in the bond-valence value of about 2.4 valence units (*vu*; A in Fig. 3). The adjacent Cu1 position, however, refined with full occupancy, does not exhibit a conspicuously large B$_{iso}$ value, thus contradicting a potentially mixed (Pb, Bi) character of the Pb1 position.

TABLE 7. CATION–ANION DISTANCES IN THE LINDSTRÖMITE COMPONENT:
COMPARISON OF RESULTS OBTAINED BY SIMULTANEOUS REFINEMENT
WITH THOSE FROM CLASSICAL REFINEMENT BY TOPA (2001)

_____

$bd_{60.1}$ **VP**

Bi1-		Bi2-		Bi3-		Bi4-		Bi5-	
S6	2.619(18)	S7	2.591(15)	S8	2.660(19)	S9	2.671(16)	S12	2.670(12)
S13	2.739(9)	S14	2.738(12)	S15	2.717(12)	S11	2.703(12)	S12	2.670(12)
S13	2.739(9)	S14	2.738(12)	S15	2.717(12)	S11	2.703(12)	S10	2.687(18)
S5	2.992(9)	S4	3.035(9)	S3	2.971(9)	S2	3.005(9)	S1	3.041(9)
S5	2.992(9)	S4	3.035(9)	S3	2.971(9)	S2	3.005(9)	S1	3.041(9)
S13	3.233(13)	S12	3.136(18)	S11	3.120(18)	S15	3.076(17)	S14	3.057(17)
S8	3.462(20)	S7	3.535(15)	S6	3.573(19)	S10	3.552(18)	S9	3.529(18)

Bi6-		Bi7-		Pb1-		Pb2-		Pb3-	
S2	2.609(17)	S1	2.609(16)	S5	2.904(16)	S4	2.918(15)	S3	2.880(15)
S9	2.780(9)	S10	2.793(12)	S1	2.906(10)	S2	2.942(11)	S3	2.967(10)
S9	2.780(9)	S10	2.793(12)	S1	2.906(10)	S2	2.942(11)	S3	2.967(10)
S4	2.975(10)	S5	3.016(10)	S6	3.013(13)	S7	3.048(9)	S8	2.989(13)
S4	2.975(10)	S5	3.016(10)	S6	3.013(13)	S7	3.048(9)	S8	2.989(13)
S14	3.438(14)	S15	3.438(14)	S11	3.137(14)	S12	3.165(14)	S13	3.282(13)
S14	3.438(14)	S15	3.438(14)	S11	3.137(14)	S12	3.165(14)	S13	3.282(13)
				S9	3.599(12)	S10	3.545(17)	S6	3.807(17)

Cu1-		Cu2-		Cu3-		Cu4-		Cu5-	
S3	2.330(17)	S4	2.316(17)	S5	2.328(18)	S10	2.288(63)	S11	2.238(83)
S6	2.354(10)	S7	2.343(7)	S8	2.354(10)	S10	2.288(63)	S1	2.285(92)
S6	2.354(10)	S7	2.343(7)	S8	2.354(10)	S2	2.343(99)	S9	2.392(40)
S13	2.413(16)	S14	2.396(18)	S15	2.382(18)	S12	2.416(99)	S9	2.392(40)

$bd_{60.1}$

Bi1-		Bi2-		Bi3-		Bi4-		Bi5-	
S6	2.677(12)	S7	2.639(11)	S8	2.677(11)	S9	2.708(11)	S12	2.693(6)
S13	2.745(6)	S14	2.743(7)	S15	2.728(7)	S11	2.719(7)	S12	2.693(6)
S13	2.745(6)	S14	2.743(7)	S15	2.728(7)	S11	2.719(7)	S10	2.702(11)
S5	2.967(8)	S4	2.996(8)	S3	2.953(7)	S2	2.985(8)	S1	3.005(7)
S5	2.967(8)	S4	2.996(8)	S3	2.953(7)	S2	2.985(8)	S1	3.005(7)
S13	3.167(9)	S12	3.092(9)	S11	3.072(10)	S15	3.034(10)	S14	3.041(10)
S8	3.460(12)	S7	3.510(12)	S6	3.524(12)	S10	3.534(12)	S9	3.505(12)

Bi6-		Bi7-		Pb1-		Pb2-		Pb3-	
S2	2.580(11)	S1	2.572(11)	S5	2.882(11)	S4	2.878(12)	S3	2.825(10)
S9	2.774(7)	S10	2.777(8)	S1	2.948(8)	S2	2.974(8)	S8	2.966(8)
S9	2.774(7)	S10	2.777(8)	S1	2.948(8)	S2	2.974(8)	S8	2.966(8)
S4	3.016(8)	S5	3.050(8)	S6	2.987(8)	S7	3.005(7)	S3	3.000(8)
S4	3.016(8)	S5	3.050(8)	S6	2.987(8)	S7	3.005(7)	S3	3.000(8)
S14	3.424(9)	S15	3.433(9)	S11	3.160(8)	S12	3.179(8)	S13	3.288(8)
S14	3.424(9)	S15	3.433(9)	S11	3.160(8)	S12	3.179(8)	S13	3.288(8)
				S9	3.652(11)	S10	3.616(11)	S6	3.833(11)

Cu1-		Cu2-		Cu3-		Cu4-		Cu5-	
S3	2.360(12)	S4	2.338(13)	S5	2.323(13)	S1	2.327(36)	S2	2.260(37)
S6	2.362(7)	S7	2.356(6)	S8	2.364(7)	S9	2.361(19)	S10	2.356(21)
S6	2.362(7)	S7	2.356(6)	S8	2.364(7)	S9	2.361(19)	S10	2.356(21)
S13	2.457(12)	S14	2.423(12)	S15	2.436(12)	S11	2.401(36)	S12	2.503(38)

_____

The marginal Bi sites Bi1 through Bi5 form tight clusters in all plots; these cations have 2.8–3.0 bond-valence units. The partly substituted, mixed (Bi, Pb) sites Bi6 and Bi7, situated between 2.6 and 2.9 *vu*, possess typical intermediate volumes of the spheres (but not similarly altered volumes of polyhedra, see Table 9) and the largest eccentricity of all large cation sites. Differences between the two lindströmite samples and between the results of simultaneous refinement and those of the conservative approach by Topa (2001) are small; only the polyhedron of Pb1, already mentioned, differs from the rest (Fig. 3).

For associated krupkaite, the results for 'bd60', 'bd64' (this study) and bd50 and bd59 (Topa *et al.* 2002b) have been plotted in Figure 4. The Pb site, with a bond-valence value close to 2 *vu*, has a sphere volume and an eccentricity similar to the corresponding sites in lindströmite. The internal Bi site of the ribbon, Bi3, differs profoundly between pure krupkaite bd50, krupkaite from 'bd60' and that from 'bd64': the sphere volume stays constant, ~115 Å³, but the bond valence is only 2.3 *vu* for Bi3 in 'bd64', being ~2.8 *vu* in other structures. Bond-valence values for Bi1 and Bi2 are consistently 2.8–3.0 *vu*.

A comparison of the three structures of krupkaite leads to the conclusion that krupkaite in 'bd$_{64}$' is over-substituted or, less probably, that we are dealing with krupkaite that contains antiphase domains, similar to the case described by Mumme (1975). In this case, both inner large-cation sites of the ribbons represent mixed (Bi, Pb) positions, albeit in very different proportions. This suggestion, however, is not in agreement with the absence of the Cu2 position and the presence of full Cu1 and Pb positions in this exsolved krupkaite. The eccentricity of the Bi3 site in 'bd$_{64}$' differs from the values observed for analogous sites Bi6 and Bi7 in lindströmite, and approaches that of Pb in the corresponding position. It differs substantially from the eccentricity value of the mixed (Bi, Pb) position in pure krupkaite (59), equal to 0.177 when a single mixed site is refined, and 0.189 and 0.095, respectively, if this site is split into 0.82 Bi and 0.18 Pb (Topa et $al.$ 2002b). Without an indication of additional Cu in the refinement results, the degree of oversubstitution cannot be evaluated.

TABLE 7 (cont'd). CATION–ANION DISTANCES IN THE LINDSTRÖMITE COMPONENT: COMPARISON OF RESULTS OBTAINED BY SIMULTANEOUS REFINEMENT WITH THOSE FROM CLASSICAL REFINEMENT BY TOPA (2001)

bd$_{64.1}$

Bi1-		Bi2-		Bi3-		Bi4-		Bi5-	
S6	2.652(10)	S7	2.611(10)	S8	2.690(10)	S9	2.672(10)	S12	2.695(7)
S13	2.745(7)	S14	2.747(7)	S15	2.728(7)	S11	2.707(7)	S12	2.695(7)
S13	2.745(7)	S14	2.747(7)	S15	2.728(7)	S11	2.707(7)	S10	2.703(11)
S5	2.992(8)	S4	3.005(8)	S3	2.941(8)	S2	3.010(8)	S1	3.002(7)
S5	2.992(8)	S4	3.005(8)	S3	2.941(8)	S2	3.010(8)	S1	3.002(7)
S13	3.215(10)	S12	3.097(10)	S11	3.077(10)	S15	3.081(10)	S14	3.024(10)
S8	3.447(9)	S7	3.535(11)	S6	3.549(11)	S10	3.544(11)	S9	3.541(11)

Bi6-		Bi7-		Pb1-		Pb2-		Pb3-	
S2	2.610(11)	S1	2.607(10)	S5	2.889(11)	S4	2.912(10)	S3	2.867(11)
S9	2.771(6)	S10	2.771(8)	S1	2.942(7)	S2	2.940(8)	S8	2.980(8)
S9	2.771(6)	S10	2.771(8)	S1	2.942(7)	S2	2.940(8)	S8	2.980(8)
S4	2.998(8)	S5	3.021(8)	S6	2.983(7)	S7	3.018(7)	S3	2.999(8)
S4	2.998(8)	S5	3.021(8)	S6	2.983(7)	S7	3.018(7)	S3	2.999(8)
S14	3.429(8)	S15	3.420(9)	S11	3.183(7)	S12	3.184(7)	S13	3.280(8)
S14	3.429(8)	S15	3.420(9)	S11	3.183(7)	S12	3.184(7)	S13	3.280(8)
				S9	3.667(9)	S10	3.622(11)	S6	3.834(10)

Cu1-		Cu2-		Cu3-		Cu4-		Cu5-	
S3	2.339(12)	S4	2.305(11)	S5	2.322(12)	S1	2.175(51)	2	2.267(47)
S6	2.362(6)	S7	2.356(6)	S8	2.355(6)	S11	2.276(**)	S10	2.378(23)
S6	2.362(6)	S7	2.356(6)	S8	2.355(6)	S9	2.512(91)	S10	2.378(23)
S13	2.425(12)	S14	2.449(12)	S15	2.393(12)	S9	2.512(91)	S12	2.410(44)

bd$_{64.1}$ VP

Bi1-		Bi2-		Bi3-		Bi4-		Bi5-	
S6	2.636(21)	S7	2.556(17)	S15	2.711(12)	S9	2.649(17)	S10	2.674(23)
S13	2.752(12)	S14	2.764(15)	S15	2.711(12)	S11	2.713(12)	S12	2.681(12)
S13	2.752(12)	S14	2.764(15)	S8	2.750(25)	S11	2.713(12)	S12	2.681(12)
S5	2.977(17)	S4	3.037(17)	S3	2.945(13)	S2	3.001(17)	S14	2.986(22)
S5	2.977(17)	S4	3.037(17)	S3	2.945(13)	S2	3.001(17)	S1	3.057(13)
S13	3.265(17)	S12	3.098(18)	S11	3.065(17)	S15	3.098(18)	S1	3.057(13)
S8	3.418(23)	S7	3.536(17)	S6	3.599(20)	S10	3.558(23)	S9	3.554(17)

Bi6-		Bi7-		Pb1-		Pb2-		Pb3-	
S2	2.554(23)	S1	2.583(19)	S5	2.822(22)	S4	2.879(21)	S3	2.848(18)
S9	2.776(12)	S10	2.791(16)	S1	2.896(13)	S2	2.963(17)	S8	2.918(20)
S9	2.776(12)	S10	2.791(16)	S1	2.896(13)	S2	2.963(17)	S8	2.918(20)
S4	2.978(16)	S5	3.037(17)	S6	2.947(17)	S7	3.094(13)	S3	2.991(13)
S4	2.978(16)	S5	3.037(17)	S6	2.947(17)	S7	3.094(13)	S3	2.991(13)
S14	3.435(16)	S15	3.426(15)	S11	3.174(14)	S12	3.167(15)	S13	3.287(14)
S14	3.435(16)	S15	3.426(15)	S11	3.174(14)	S12	3.167(15)	S13	3.287(14)
				S9	3.611(17)	S10	3.534(23)	S6	3.901(22)

Cu1-		Cu2-		Cu3-		Cu4-		Cu5-	
S3	2.377(20)	S7	2.321(9)	S15	2.360(20)	S10	2.272(24)	S1	2.168(39)
S13	2.394(19)	S7	2.321(9)	S8	2.378(15)	S10	2.272(24)	S9	2.403(21)
S6	2.395(13)	S4	2.354(21)	S8	2.378(15)	S2	2.412(52)	S9	2.403(21)
S6	2.395(13)	S14	2.460(22)	S5	2.436(24)	S12	2.497(49)	S11	2.503(38)

Note that 'bd$_{nn}$' indicates a bulk electron-microprobe-derived composition of the intergrowth studied. VP: results of the present, simultaneous refinement; no code: classical refinement by Topa (2001).

TABLE 8. CATION–ANION DISTANCES IN THE KRUPKAITE COMPONENT:
COMPARISON WITH THE VALUES FOR PURE KRUPKAITE

bd_{50} VP

Bi1-		Bi2-		Bi3-		Pb1-		Cu1-	
S6	2.706(22)	S3	2.698(23)	S5	2.607(23)	S4	2.870(23)	S4	2.316(26)
S2	2.718(14)	S1	2.743(14)	S6	2.742(14)	S3	2.970(15)	S3	2.373(12)
S2	2.718(14)	S1	2.743(14)	S6	2.742(14)	S3	2.970(15)	S3	2.373(12)
S5	2.962(15)	S4	2.988(16)	S4	3.017(16)	S5	2.992(16)	S1	2.479(24)
S5	2.962(15)	S4	2.988(16)	S4	3.017(16)	S5	2.992(16)		
S1	3.041(20)	S2	3.087(21)	S1	3.439(19)	S2	3.189(18)		
S6	3.543(23)	S3	3.464(25)	S1	3.439(19)	S2	3.189(18)		
						S6	3.744(21)		

bd_{50}

Bi1-		Bi1-		Bi1-		Pb1-		Cu1-	
S2	2.686(5)	S3	2.654(7)	S5	2.585(7)	S4	2.908(7)	S4	2.317(8)
S2	2.686(5)	S1	2.731(5)	S6	2.760(5)	S5	2.944(5)	S3	2.350(5)
S6	2.712(7)	S1	2.731(5)	S6	2.760(5)	S5	2.944(5)	S3	2.350(5)
S5	3.014(5)	S4	3.009(5)	S4	2.998(5)	S3	3.001(6)	S1	2.418(8)
S5	3.014(5)	S4	3.009(5)	S4	2.998(5)	S3	3.001(6)		
S1	3.051(7)	S2	3.121(7)	S1	3.457(6)	S2	3.164(5)		
S6	3.520(7)	S3	3.484(7)	S1	3.457(6)	S2	3.164(5)		
						S6	3.638(7)		

bd_{50} 2 VP

Bi1-		Bi2-		Bi3-		Pb1-		Cu1-	
S6	2.666(27)	S3	2.685(23)	S5	2.767(23)	S4	2.879(27)	S4	2.226(35)
S2	2.705(15)	S1	2.705(23)	S6	2.865(24)	S3	2.940(17)	S1	2.389(45)
S2	2.705(15)	S1	2.705(23)	S6	2.865(24)	S3	2.940(17)	S3	2.401(21)
S5	2.940(15)	S4	3.046(25)	S4	2.934(23)	S5	2.991(16)	S3	2.401(21)
S5	2.940(15)	S4	3.046(25)	S4	2.934(23)	S5	2.991(16)		
S1	3.093(34)	S2	3.145(23)	S1	3.355(29)	S2	3.231(19)		
S6	3.522(23)	S3	3.501(24)	S1	3.355(29)	S2	3.231(19)		
						S6	3.746(33)		

Note that bd_{50} VP and bd_{50} 2-VP indicate data from the samples '$bd_{60.1}$' and '$bd_{64.1}$', respectively. Data without a code pertain to pure krupkaite (Topa *et al.* 2002).

Mass balance

A *semiquantitative* check of data obtained can be performed by calculations of the percentage of aikinite in the minor phase, krupkaite, using the electron-microprobe data for the average composition of the submicroscopic intergrowth, the structure-derived composition of the lindströmite component, and the volume ratio of the two phases refined. In these calculations, we assume the same volume of the 11.5 Å subcell of both components, which is nearly true for the two phases examined, which are so close chemically.

For the bulk composition $bd_{60.1}$, with the lindströmite : krupkaite volume ratio equal to 0.662/0.337

$$1 \times 60.1\% = 0.662 \times 62.62\% + 0.337 \times X\%$$

$$X = 55.14\%$$

Thus, the approximate percentage X of aikinite in the the krupkaite portion of the intergrowth should be 55.1%, which lies within a 10% deviation from that suggested by the structure analysis. If the exsolved krupkaite is assumed to be bd_{50}, as determined by the structure refinement,

$$1 \times 60.1\% = 62.62 \text{ y} + 50.0 \text{ (1–y)}$$

$$y = 0.800$$

so that lindströmite $bd_{62.6}$ should account for 80 vol.%, whereas krupkaite bd_{50} should account for 20 vol.%.

In an analogous way, for the bulk composition $bd_{64.1}$, the observed volume-ratio of 0.625/0.375 and the structurally determined composition of lindströmite (equal to $bd_{66.4}$) lead to the suggestion of oversubstitution in exsolved krupkaite, this being equal to $bd_{60.3}$. If krupkaite (bd_{50}) is assumed instead, these calculations result in 86.1 vol.% lindströmite ($bd_{66.4}$) and 13.9 vol.% krupkaite (bd_{50}).

Quality of the refinements

To summarize, the simultaneous refinement of the two cases of lindströmite–krupkaite intergrowth examined yields on the one hand a crystal structure of

TABLE 9. POLYHEDRON CHARACTERISTICS FOR CATION COORDINATION POLYHEDRA IN THE LINDSTRÖMITE COMPONENT

1	2	3	4	5	6	7	8	9	10
				bd$_{69.1}$ VP					
Bi1	2.975	0.1557	0.986	0.1038	0.3982	0.959	110.268	37.396	2.878
Bi2	2.979	0.1627	0.985	0.104	0.4129	0.9538	110.713	37.538	2.913
Bi3	2.964	0.1599	0.969	0.1036	0.4071	0.9081	109.059	36.992	2.935
Bi4	2.961	0.1577	0.972	0.1078	0.4025	0.9173	108.734	36.711	2.936
Bi5	2.957	0.1602	0.976	0.1042	0.4078	0.9291	108.345	36.725	2.992
Bi6	3.011	0.175	0.979	0.1268	0.4385	0.9364	114.293	37.767	2.742
Bi7	3.025	0.1742	0.983	0.1235	0.4368	0.9502	115.938	38.453	2.639
Pb1	3.068	0.0925	0.95	0.0401	0.2525	0.8485	120.924	50.315	2.189
Pb2	3.088	0.0841	0.958	0.0373	0.2316	0.8741	123.334	51.469	2.031
Pb3	3.125	0.132	0.946	0.0422	0.346	0.8386	127.789	53.053	1.979
Cu1	2.359	0.023	1	0.0255	0.0674	0.9995	54.967	6.562	1.031
Cu2	2.343	0.0245	0.998	0.0366	0.0717	0.9952	53.91	6.363	1.069
Cu3	2.351	0.0174	0.996	0.0278	0.0514	0.9892	54.415	6.482	1.052
Cu4	2.328	0.0434	0.999	0.0278	0.1246	0.9979	52.883	6.299	1.123
Cu5	2.329	0.056	1	0.0234	0.1587	0.9996	52.929	6.333	1.152
				bd$_{60.1}$					
Bi1	2.966	0.144	0.980	0.098	0.372	0.940	109.346	37.305	2.812
Bi2	2.965	0.151	0.979	0.099	0.388	0.936	109.214	37.221	2.878
Bi3	2.951	0.149	0.970	0.098	0.383	0.909	107.592	36.735	2.935
Bi4	2.957	0.148	0.969	0.101	0.382	0.907	108.335	36.854	2.877
Bi5	2.952	0.150	0.974	0.100	0.387	0.923	107.718	36.682	2.948
Bi6	3.016	0.179	0.985	0.130	0.447	0.955	114.969	37.838	2.770
Bi7	3.028	0.182	0.988	0.128	0.453	0.964	116.292	38.364	2.727
Pb1	3.080	0.105	0.952	0.037	0.283	0.855	122.418	51.112	2.139
Pb2	3.091	0.100	0.958	0.035	0.270	0.874	123.736	51.736	2.054
Pb3	3.126	0.145	0.950	0.039	0.375	0.849	127.908	53.277	2.021
Cu1	2.381	0.032	1.000	0.021	0.092	0.999	56.551	6.783	0.973
Cu2	2.363	0.027	0.999	0.029	0.079	0.996	55.242	6.569	1.017
Cu3	2.366	0.032	0.999	0.023	0.092	0.996	55.473	6.638	1.009
Cu4	2.360	0.019	1.000	0.019	0.055	1.000	55.050	6.616	1.031
Cu5	2.358	0.063	1.000	0.024	0.178	1.000	54.909	6.565	1.039

1	2	3	4	5	6	7	8	9	10
				bd$_{64.1}$ VP					
Bi1	2.98	0.15	0.99	0.1	0.38	0.96	110.38	37.44	2.82
Bi2	2.98	0.16	0.98	0.1	0.41	0.95	110.51	37.63	2.94
Bi3	2.96	0.15	0.96	0.1	0.39	0.87	108.97	37.16	2.87
Bi4	2.97	0.16	0.98	0.11	0.41	0.93	109.25	36.94	2.94
Bi5	2.96	0.16	0.97	0.1	0.42	0.92	108.28	36.95	3
Bi6	3.01	0.18	0.98	0.14	0.46	0.96	114.11	37.36	2.89
Bi7	3.03	0.18	0.99	0.13	0.44	0.97	116.34	38.43	2.68
Pb1	3.05	0.12	0.96	0	0.31	0.87	118.75	49.54	2.38
Pb2	3.1	0.1	0.96	0	0.23	0.88	124.98	52.27	1.97
Pb3	3.12	0.16	0.94	0	0.4	0.83	127.04	52.82	2.09
Cu1	2.39	0	1	0	0	1	57.147	6.84	0.95
Cu2	2.35	0.1	1	0	0.15	1	54.57	6.445	1.04
Cu3	2.39	0	1	0	0.1	0.99	57.205	6.852	0.96
Cu4	2.35	0.1	1	0	0.23	1	54.67	6.509	1.06
Cu5	2.35	0.1	1	0	0.24	1	54.554	6.538	1.07
				bd$_{64.1}$					
Bi1	2.98	0.15	0.99	0.1	0.38	0.96	110.25	37.47	2.8
Bi2	2.97	0.16	0.98	0.1	0.4	0.94	109.54	37.36	2.91
Bi3	2.95	0.15	0.97	0.1	0.39	0.9	107.93	36.76	2.92
Bi4	2.96	0.16	0.97	0.1	0.4	0.92	108.88	36.99	2.91
Bi5	2.95	0.15	0.97	0.1	0.4	0.91	107.88	36.78	2.95
Bi6	3.02	0.18	0.98	0.13	0.44	0.94	114.88	37.8	2.73
Bi7	3.02	0.17	0.98	0.13	0.44	0.95	114.98	38.01	2.71
Pb1	3.09	0.11	0.95	0	0.29	0.85	122.98	51.3	2.12
Pb2	3.09	0.1	0.95	0	0.26	0.86	123.9	51.69	2.05
Pb3	3.13	0.14	0.95	0	0.36	0.84	128.47	53.42	1.95
Cu1	2.37	0	1	0	0.1	1	55.634	6.661	1.01
Cu2	2.36	0	1	0	0.11	1	54.891	6.53	1.03
Cu3	2.35	0.018	1	0	0.1	1	54.551	6.519	1.05
Cu4	2.36	0.12	1	0	0.31	1	54.908	6.591	1.1
Cu5	2.35	0	1	0	0.11	1	54.592	6.543	1.05

For detailed explanation of polyhedron characteristics see Makovicky *et al.* (2001) or Topa *et al.* (2003, Appendix). For sample codes, see Table 7. Column headings: 1: atom, 2: sphere radius (Å), 3: eccentricity, 4: sphericity, 5: epsilon, 6: volume eccentricity, 7: volume sphericity, 8: sphere volume (Å^3), 9: polyhedron volume (Å^3), 10: valence.

TABLE 10. POLYHEDRON CHARACTERISTICS FOR CATION POLYHEDRA IN THE KRUPKAITE COMPONENT

1	2	3	4	5	6	7	8	9	10
				bd50 VP					
Bi1	2.953	0.151	0.967	0.098	0.388	0.901	107.888	36.844	2.916
Bi2	2.962	0.138	0.978	0.094	0.359	0.935	108.841	37.303	2.788
Bi3	3.020	0.182	0.979	0.136	0.453	0.936	115.342	37.720	2.795
Pb1	3.101	0.121	0.950	0.036	0.321	0.850	124.941	52.203	2.065
Cu1	2.377	0.044	1.000	0.021	0.126	1.000	56.241	6.749	0.979
				bd50					
Bi1	2.956	0.153	0.973	0.102	0.393	0.920	108.186	36.777	2.932
Bi2	2.966	0.149	0.982	0.099	0.383	0.946	109.286	37.263	2.853
Bi3	3.014	0.186	0.979	0.128	0.460	0.938	114.689	37.831	2.812
Pb1	3.085	0.099	0.952	0.037	0.269	0.855	122.955	51.325	2.094
Cu1	2.353	0.028	1.000	0.027	0.083	1.000	54.554	6.506	1.044
				bd50_2 VP					
Bi1	2.943	0.153	0.970	0.105	0.392	0.909	106.778	36.175	3.046
Bi2	2.977	0.154	0.981	0.101	0.395	0.944	110.485	37.604	2.811
Bi3	3.023	0.124	0.976	0.125	0.329	0.929	115.685	38.304	2.345
Pb1	3.097	0.126	0.951	0.040	0.333	0.853	124.392	51.784	2.072
Cu1	2.349	0.052	1.000	0.021	0.149	1.000	54.263	6.512	1.075

For explanations and sample codes, see Tables 9 and 8, respectively.

slightly oversubstituted lindströmite (bd$_{62.6}$) with three fully and two unevenly, partly occupied tetrahedral Cu sites, which is intergrown with krupkaite (bd$_{\sim50}$), and on the other hand, oversubstituted lindströmite (bd$_{\leq66.3}$) which has the same types of Cu positions, intergrown with oversubstituted krupkaite (bd$_{\leq60}$). The latter values represent the calculated upper limits, and they are probably too high. They may be artefacts of a refinement based on somewhat inferior intensity-data (see Table 2) resulting from the texture of the 'bd$_{64}$' intergrowth. An evaluation of our results suggests that the simultaneous refinement of two closely related, regularly intergrown structures yields data of a good quality, adequate for a detailed analysis of the polyhedra in the resulting structures. The occupancies of fractionally occupied sites, however, are very sensitive to the quality of the diffraction data, because of the high correlations between two very similar structures, with considerably overlapping reciprocal lattices.

Origin of aggregates

Our observation of the intimate krupkaite – lindströmite intergrowths (Topa *et al.* 2002a), backed also by literature data (Horiuchi & Wuensch 1977, Pring & Hyde 1987), leads us to a model of oversubstituted krupkaite exsolving into an intimate aggregate of two ordered phases, lindströmite and a stoichiometric or less oversubstituted krupkaite. From a model of simple exsolution (under a process of ordering), one would expect a somewhat oversubstituted krupkaite and undersubstituted lindströmite, reaching ideal composi-

tions with time and decreasing temperature. Instead, at least for "lindströmite" (bd$_{60}$), the structure analysis indicates krupkaite (bd$_{50}$) associated with oversubstituted lindströmite. We consider the thermodynamic stability of stoichiometric krupkaite (bd$_{50}$), as suggested by its behavior in the complex exsolution processes in the aikinite–bismuthinite series (Topa *et al.* 2002a), as one of the potential factors in Cu–Pb distribution between the exsolved phases. We explain the tendency of lindströmite to show oversubstitution by the same mechanism as proposed for salzburgite (Topa *et al.* 2000) and emilite (Balić-Žunić *et al.* 2002). It is based on the metric misfit of pure aikinite modules (*a* 4.042Å, *b* 11.652 Å) and pure krupkaite modules (*a* 4.015 Å, *c* 11.560 Å). Periodic alternation, along *b*, of these two modules in one structure requires a mutual adjustment of their size. The best adjustment of the smaller module (krupkaite) to the size that can then be accom-

modated by strain adjustments to the aikinite module, is to absorb more Cu and Pb than dictated by a simple stoichiometric formula with full and empty tetrahedra, and appropriately occupied adjacent (Pb,Bi) sites. In the case of "lindströmite (bd$_{64}$)", not only lindströmite but, according to the Bi3 coordination data and calculations of stoichiometry, also the associated krupkaite appears to be oversubstituted or disordered, or both.
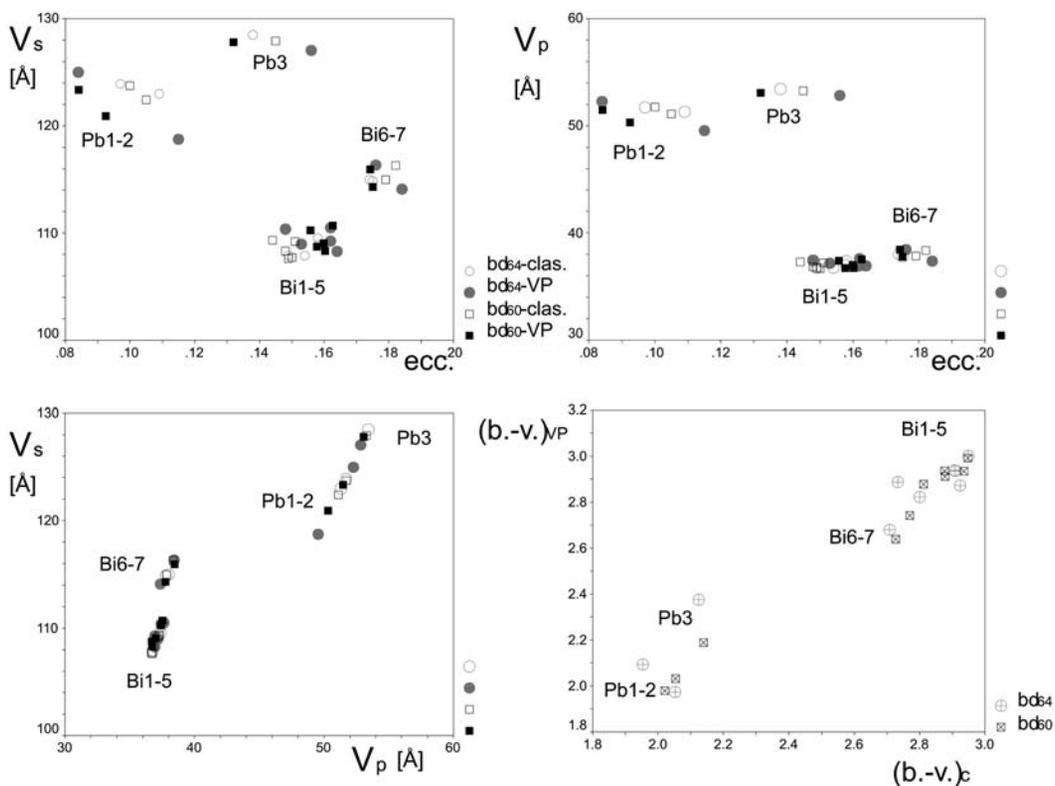
FIG. 3. Correlation of polyhedron characteristics for the large cations in lindströmite. Cation eccentricity, volume of circumscribed sphere and of the coordination polyhedron itself are cross-correlated. Labeling indicates cation types in question (see text). Bond-valence values obtained from the results of simultaneous refinement are compared with those obtained from classical refinement by Topa (2001). Sample codes as in Table 7.
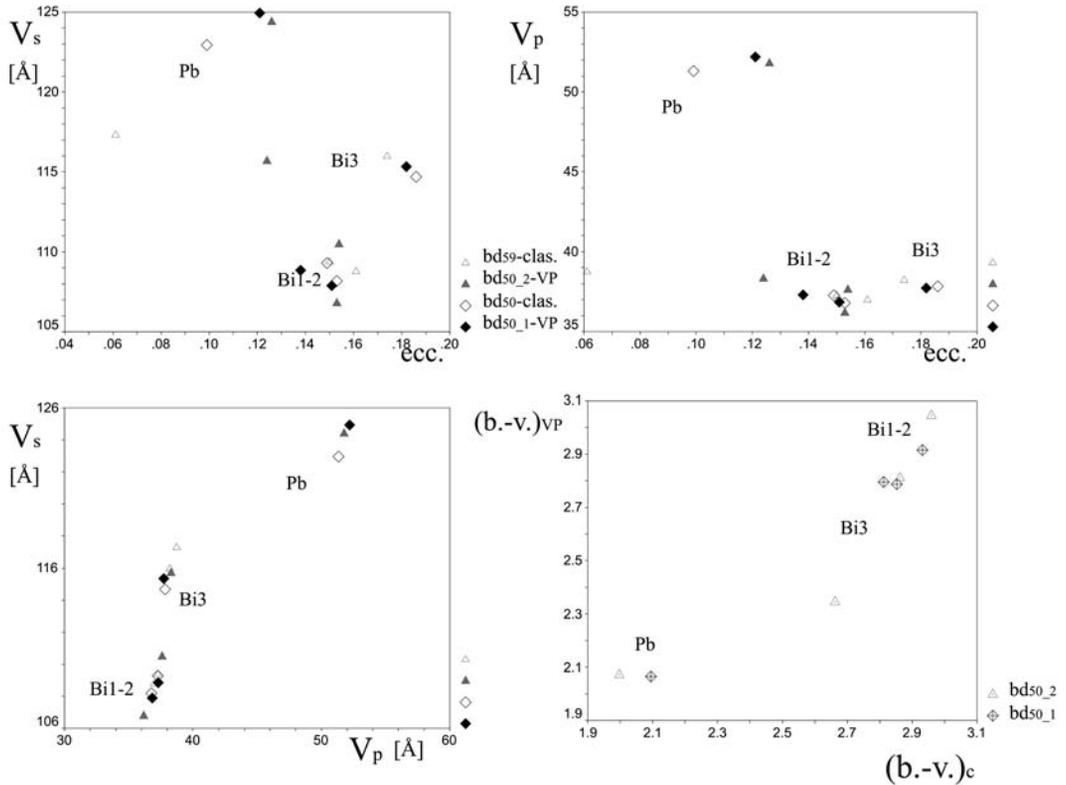
FIG. 4.   Correlation of polyhedron characteristics for large cations in krupkaite. For details see figure caption of Figure 3 and Table 8.

REFERENCES

BALIĆ-ŽUNIĆ, T. & MAKOVICKY, E. (1996): Determination of the centroid or the 'best centre' of a coordination polyhedron. *Acta Crystallogr.* **B52**, 78-81.

BALIĆ-ŽUNIĆ, T., TOPA, D. & MAKOVICKY, E. (2002): The crystal structure of emilite, $Cu_{10.7}Pb_{10.7}Bi_{21.3}S_{48}$, the second 45 Å derivative of the bismuthinite–aikinite solid-solution series. *Can. Mineral.* **40**, 239-245.

BRESE, N.E.& O'KEEFFE, M. (1991): Bond-valence parameters for solids. *Acta Crystallogr.* **B47**, 192-197.

HORIUCHI, H. & WUENSCH, B.J. (1977): Lindströmite, $Cu_3Pb_3Bi_7S_{15}$: its space group and ordering scheme for metal atoms in the crystal structure. *Can. Mineral.* **15**, 527-535.

MAKOVICKY, E. & BALIĆ-ŽUNIĆ, T. (1998): New measure of distortion for coordination polyhedra. *Acta Crystallogr.* **B54**, 766-773.

MAKOVICKY, E. & MAKOVICKY, M. (1978): Representation of compositions in the bismuthinite–aikinite series. *Can. Mineral.* **16**, 405-409.

MAKOVICKY, E. & SKINNER B.J. (1979): Studies of the sulfosalts of copper. VII. Crystal structures of the exsolution products $Cu_{12..3}Sb_4S_{13}$ and $Cu_{13..8}Sb_4S_{13}$ of unsubstituted synthetic tetrahedrite. *Can. Mineral.* **17**, 619-634.

MAKOVICKY, E., TOPA, D. & BALIĆ-ŽUNIĆ, T. (2001): The crystal structure of paarite, the newly discovered 56 Å derivative of the bismuthinite–aikinite solid-solution series. *Can. Mineral.* **39**, 1377-1382.

MUMME, W.G. (1975): The crystal structure of krupkaite, $CuPbBi_3S_6$, from the Juno mine, at Tennant Creek, Northern Territory, Australia. *Am. Mineral.* **60**, 300-308.

MUMME, W.G., WELIN, E. & WUENSCH, B.J. (1976): Crystal chemistry and proposed nomenclature for sulfosalts intermediate in the system bismuthinite–aikinite (Bi_2S_3–$CuPbBiS_3$). *Am. Mineral.* **61**, 15-20.

OHMASA, M. & NOWACKI, W. (1970): Note on the space group and on the structure of aikinite derivatives. *Neues Jahrb. Mineral., Monatsh.*, 158-162.

PETŘÍČEK, V., DUŠEK, M. & PALATINUS, L. (2000): JANA2000. www-xray.fzu.cz/jana/jana2000.

POST, J.E. & BISH, D.L. (1989): Rietveld refinement of crystal structures using powder X-ray diffraction data. *In* Modern Powder Diffraction (D.L. Bish & J.E. Post, eds.). *Rev. Mineral.* **20**, 277-308.

PRING, A., GRGURIC, B.A. & CRIDDLE, A.J. (1998): Lindströmite from Cobalt, Ontario. *Can. Mineral.* **36**, 1139-1148.

PRING, A.& HYDE, B.G. (1987): Structural disorder in lindströmite: a bismuthinite – aikinite derivative. *Can. Mineral.* **25**, 393-399.

SPRINGER, G. (1971): The synthetic solid-solution series Bi_2S_3–$BiCuPbS_3$ (bismuthinite–aikinite). *Neues Jahrb. Mineral., Monatsh.*, 13-24.

TOPA, D. (2001): *Mineralogy, Crystal Structure and Crystal Chemistry of the Bismuthinite–Aikinite Series from Felbertal, Austria*. Doctoral thesis, Institute of Mineralogy, Natural Science Faculty of the Paris-Lodron-University of Salzburg, Salzburg, Austria.

TOPA, D., BALIĆ-ŽUNIĆ, T. & MAKOVICKY, E. (2000): The crystal structure of $Cu_{1.6}Pb_{1.6}Bi_{6.4}S_{12}$, a new 44.8 Å derivative of the bismuthinite–aikinite solid-solution series. *Can. Mineral.* **38**, 611-616.

TOPA, D., MAKOVICKY, E. & BALIĆ-ŽUNIĆ, T. (2002b): The structural role of excess Cu and Pb in gladite and krupkaite based on new refinements of their structure. *Can. Mineral.* **40**, 1147-1159.

TOPA, D., MAKOVICKY, E. & BALIĆ-ŽUNIĆ, T. (2003): Crystal structures and crystal chemistry of members of the cuprobismutite homologous series of sulfosalts. *Can. Mineral.* **41**, 1481-1501.

TOPA, D., MAKOVICKY, E. & PAAR, W.H. (2002a): Composition ranges and exsolution pairs for the members of the bismuthinite–aikinite series from Felbertal, Austria. *Can. Mineral.* **40**, 849-869.

ŽÁK, L., SYNEČEK, V. & HYBLER J. (1974): Krupkaite, $CuPbBi_3S_6$, a new mineral of the bismuthinite–aikinite group. *Neues Jahrb. Mineral., Monatsh.*, 533-541.